Transcriptional profiling reveals mechanisms of sexually dimorphic responses of *Populus cathayana* to potassium deficiency

Qingquan Han [a, b], Haifeng Song [a,b], Yanni Yang [a], Hao Jiang [a], Sheng Zhang [a, *]

[a] Key Laboratory of Mountain Surface Processes and Ecological Regulation, Institute of Mountain Hazards and Environment, Chinese Academy of Sciences, Chengdu 610041, China

[b] University of Chinese Academy of Sciences, Beijing 100039, China

* Correspondence address:

Sheng Zhang

Key Laboratory of Mountain Surface Processes and Ecological Regulation, Institute of Mountain Hazards and Environment, Chinese Academy of Sciences, Chengdu 610041, China

Correspondence

Corresponding author, e-mail: zhangsheng@imde.ac.cn

Potassium (K) deficiency causes a series of physiological and metabolic disorders in plants, and dioecious species exhibit different responses based on gender. Our previous morphological and physiological observations indicated that *Populus cathayana* males were more tolerant to K^+ deficiency than females. To continue this work, comparative transcriptome analyses were carried out to investigate sexually differential expressed genes (DEGs) in this study. The results indicate that 10 weeks of K^+ deficiency result in 111 and 181 DEGs in males and females, respectively. These DEGs are mainly involved in photosynthesis, cell wall biosynthesis, secondary metabolism, transport, stress responses, gene expression regulation and protein synthesis and degradation. Comparison between sexes, *P. cathayana* females showed more changes in response to K^+ deficiency than males with regard to photosynthesis, gene expression regulation and posttranslational modification but fewer changes in secondary metabolism, stress responses and redox homeostasis. These results provide evidence that *P. cathayana* females are more susceptible to K^+ deficiency than males. Therefore, there are gender-related molecular strategies in response to K^+ deficiency between sexes.

Key words: Transcriptional profiling, sexual differences, potassium deficiency, poplar

Abbreviations - P_n, net photosynthesis rate; g_s, stomatal conductance; E, transpiration rate; C_i, intercellular CO_2 concentration; *Chl*, chlorophyll; *TChl*, total chlorophyll; *Caro*, carotenoid; F_v/F_m, maximum efficiency of PSII; Yield, maximum effective quantum yield of PSII; *qP*, photochemical quenching coefficient; *qN*, non-photochemical quenching coefficient; SOD, superoxide dismutase; POD,

This article has been accepted for publication and undergone full peer review but has not been through the copyediting, typesetting, pagination and proofreading process, which may lead to differences between this version and the Version of Record. Please cite this article as doi: 10.1111/ppl.12636

peroxidase; APX, ascorbate peroxidase; CAT, catalase; DEGs, differentially expressed genes; MC, control males; FC, control females; MK, K^+-deficient males; FK, K^+-deficient females; qRT-PCR, quantitative real-time polymerase chain reaction.

Introduction

As an essential macronutrient for plants, potassium (K) participates in many physiological and metabolic processes, *e.g*. photosynthesis, ion transport, redox and signal transduction (Jin et al. 2011, Wang and Wu 2013, Shin and Adams 2014). Poplar is a perennial woody plant that often suffers from nutrient limitation, including K^+ deficiency. Previous studies on poplar under K^+ limitation have focused on physiological and biochemical responses. For example, Lee and Kim (2009) reported that low K^+ content in soils led to a significant decrease of K^+ concentration in roots, stems and leaves. Meanwhile, K^+ limitation increased sodium (Na^+) concentration, especially in poplar roots, causing an imbalance of Na^+: K^+ ratio (Li et al. 1990). Arend et al. (2004) studied the effect of K^+ deficiency on the plasma membrane H-ATPase, and found an enhancement of net H^+ efflux in young poplar stems. K^+ deficiency also strongly affects mesophyll conductance and chloroplast ultrastructure in poplar leaves (Houman et al. 1991, Lu et al. 2016). At transcriptional level, Ma et al. (2012) investigated the transcript profiling of rice roots in response to low-K^+ stress, and found that the differential expressed genes (DEGs) were mainly involved in metabolic process, membrane, cation binding, kinase activity and transport categories. A transcriptional analysis on K^+-deficient soybean suggested that DEGs related to oxidative stress, carbohydrate and energy metabolism, K^+ channels and ion transporters were existed (Wang et al. 2012). Additionally, Kim et al. (2012) indicated that the transcription factor RAP2.11 regulated AtHAK5 (the high-affinity K^+ uptake transporter) expression through the regulation of other genes on low-K^+ *Arabidopsis*. However, the exact molecular mechanism by which poplars responding to K^+ deficiency at the transcriptomic level remains unknown.

Poplar is a dioecious woody species. Since its fast growth, strong adaptability and less genome size, poplar is usually used as a model tree in forest research. *Populus cathayana* Rehd., mainly distributes in north, northwest and southwest of China. It shows a sex-related distribution in nature that males are more individuals in nutrient-poor habitats while females are more in nutrient-rich habitats (Xu et al. 2008, Zhao et al. 2011). Many previous studies have reported that *P. cathayana* males suffered from less growth and physiology inhibition than did females under stressed conditions. For instance, Zhang et al. (2014, 2016a) and Feng et al. (2014) showed that *P. cathayana* females displayed greater sensitivity to nitrogen (N) and phosphorus (P) deficiencies than males. In particular, Yang et al. (2015) reported that under a 30-day K^+ deficiency, *P. cathayana* males suffered less negative effects than females and showed a better resistance to K^+ limitation. K^+-deficient males exhibited higher foliar K^+ concentration and K^+: Na^+ ratio than K^+-deficient females. Additionally, *P. cathayana* males allocated more carbohydrates to roots, whereas females allocated more to leaves under K^+-deficient conditions. These results clearly demonstrate that there is sexually differential adaptive mechanism to K^+ deficiency. However, the details of sexually differential gene expression are still unknown. Therefore, to elucidate the sex-specific molecular mechanism of poplar in response to K^+ deficiency, a transcriptomic analysis was performed

in this study. Our goal was to investigate the sex-specific gene expressed profiles in *P. cathayana* males and females under K^+ deficiency.

Materials and methods

Plant materials and experimental design

Two male and female trees of *P. cathayana* collected from a natural population that located in riparian and flat valley habitats (Datong, 36°56′N, 101°35′E) in Qinghai Province, China, were used for a controlled intraspecific cross (Zhang et al. 2014). The F_1 individuals (10 males and 10 females) were vegetatively propagated to produce 40 male and 40 female bare-rooted stem cuttings, respectively. The experiment was a completely randomized design with two sexes (male and female) and two K^+ levels (control and K^+ deficiency). All cuttings were first cultivated in Hoagland's solution in a greenhouse with a daytime temperature of 19-28 °C, a night-time temperature of 12-18 °C and a relative humidity of 40-85%. The greenhouse was constructed with glass walls and transmitted approximately 82% of the natural sunlight. Each plant was grown in a separate plastic pot containing 10 l of nutrient solution. The Hoagland's solution was composed of 1.25 m*M* KNO_3, 1.25 m*M* $Ca(NO_3)_2{\cdot}4H_2O$, 0.5 m*M* $MgSO_4{\cdot}7H_2O$, 0.25 m*M* KH_2PO_4, 11.6 μ*M* H_3BO_3, 4.6 μ*M* $MnCl_2{\cdot}4H_2O$, 0.19 μ*M* $ZnSO_4{\cdot}7H_2O$, 0.12 μ*M* $Na_2MoO_4{\cdot}2H_2O$, 0.08 μ*M* $CuSO_4{\cdot}5H_2O$ and 10 μ*M* Fe supplied as Fe(III)-EDTA , and the pH was adjusted to 5.5 ± 0.2 with 0.1 *M* HCl and 0.1 *M* NaOH (Zhang et al. 2016a). Two months later, half of the cuttings (~30 cm in height) were randomly selected for K^+ deficiency treatment, in which KNO_3 was replaced by an equivalent amount of NH_4NO_3. KH_2PO_4 was replaced by an equivalent amount of $NH_4H_2PO_4$. The pH value was kept in 5.5 ± 0.2. The nutrition solution was continuously aerated and changed every three days. After 10 weeks of treatment, five cuttings of each treatment were randomly selected, and the 4th and 5th fully expanded leaves (counted from the top of the plant) were collected for physiological analyses and mRNA extraction.

Gas exchange measurements

Gas exchange measurements were conducted between 08:00 and 11:30 am using an LI-6400 portable photosynthesis system (LI-COR Inc., Lincoln, NE). Five cuttings (the fourth fully expanded and intact leaves) of each sex per treatment were randomly selected for gas exchange. A standard LI-COR leaf chamber (2 × 3 cm^2) was used. The optimal parameters were as follows: leaf temperature 25 °C, relative air humidity 60%, CO_2 concentration 400 ± 5 μmol mol^{-1}, leaf-to-air vapor pressure deficit 1.5 ± 0.5 kPa and photosynthetic photon flux density (DP) 1500 μmol m^{-2} s^{-1}, which was near to the ambient environment in the greenhouse. Before recorded, the leaves were equilibrated under the measured condition to achieve full photosynthetic induction. Once the steady-state gas exchange rates were

observed under these conditions, the net photosynthetic rate (P_n), stomatal conductance (g_s), transpiration rate (E) and intercellular CO_2 concentration (C_i) were recorded.

Chlorophyll fluorescence and leaf pigment measurements

Leaves that were used for gas exchange measurements were selected for chlorophyll fluorescence measurements using a PAM chlorophyll fluorometer (PAM 2500, Walz, Effeltrich, Germany). Before measurement, the leaf samples were placed in the dark for 30 min by covering with aluminum foil, and the minimum fluorescence yield (F_o) was recorded. Then, a saturating white light pulse of 8000 μmol m^{-2} s^{-1} was applied for 0.8 s to measure the maximum fluorescence yield (F_m). The leaves were illuminated with actinic light at an intensity of 250 μmol m^{-2} s^{-1}, which was consistent with the light intensity inside the greenhouse, and a saturating white light pulse was again applied to measure the light adapted maximum fluorescence yield (F_m'). The actinic light was then switched off, and the leaf was illuminated for 3 s with far-red light to determine the minimal fluorescence yield (F_o'). Chlorophyll fluorescence kinetics parameters were measured and calculated as described by van Kooten and Snel (1990).

For chlorophyll pigment measurements, leaf disks 0.8 cm in diameter were extracted in 80% chilled acetone (v/v) in darkness until the leaf turned white. The absorbance of the extracts was measured using a spectrophotometer (Unicam UV-330; Unicam, Cambridge, UK) at 470, 646 and 663 nm. The contents of chlorophyll a (*chl a*), chlorophyll b (*chl b*) and carotenoid (*Caro*) were calculated using the following formulae: *Chl* a= $12.21OD_{663}$-$2.81OD_{646}$; *Chl* b= $20.13OD_{646}$-$5.03OD_{663}$; *Caro*= ($1000OD_{470}$-3.27*Chl* a-104*Chl* b) /229 (Porra et al. 1989).

Enzyme activity assays

Five cuttings were randomly selected from per treatment for enzymatic activity assays of superoxide dismutase (SOD), peroxidase (POD), ascorbate peroxidase (APX), and catalase (CAT). Samples (0.5 g fresh leaves) were ground in liquid nitrogen and extracted with 50 m*M* potassium phosphate buffer (pH 7.8) containing 0.1 m*M* EDTA, 1% (w/v) PVP, 0.1 m*M* PMSF and 0.2% (v/v) Triton X-100. The resulting slurry was centrifuged at 12,000 *g*, 4 °C for 15 min, and the supernatants were used for enzyme activity assays. All operations were performed at 0-4 °C.

SOD activity was determined by measuring inhibition of the photochemical reduction of nitroblue tetrazolium (NBT), as described by Chen et al. (2011). The reaction mixture, with a total volume of 3 ml, contained 0.1 ml supernatant, 0.5 ml 600 μ*M* NBT, 1.5 ml extraction buffer and 0.3 ml of a mixture of 20 μ*M* riboflavin, 0.1 m*M* EDTA and 150 m*M* L-methionine. The reaction was initiated by the

addition of riboflavin and was carried out for 30 min under the irradiance of 170 μmol m^{-2} s^{-1} provided by a white fluorescent lamp. A system devoid of enzyme extract served as the negative control. SOD activity was measured at 560 nm, and one unit of SOD activity was defined as the amount of enzyme required to cause 50% inhibition of NBT reduction. POD activity was assayed at 436 nm in 2 ml of 100 m*M* potassium phosphate buffer (pH 6.0) containing 40 m*M* guaiacol, 10 m*M* H_2O_2, and enzyme extract containing 100 μg protein. Activity was based on the rate of tetraguaiacol production using an extinction coefficient of 25.5 mM^{-1} cm^{-1} (Chance and Maehly 1955). APX activity was measured as described by Duan et al. (2007). The reaction mixture contained enzyme extract, 50 m*M* potassium phosphate buffer (pH 7.0), 0.1 m*M* EDTA, 0.1 m*M* sodium ascorbate and 2.5 m*M* H_2O_2. Estimation of APX activity was based on the rate of oxidized ascorbate production, as derived from absorbance at 290 nm for 3 min using a spectrophotometer (UV-2450, Shimadzu, Kyoto, Japan). CAT activity was detected at 240 nm in 3 ml of 50 m*M* potassium phosphate buffer (pH 7.8) with 3 m*M* H_2O_2 and enzyme extract containing 100 μg proteins. Activity was calculated from the initial rate of the reaction using an extinction coefficient of H_2O_2 of 40 mM^{-1} cm^{-1} at 240 nm. One unit of CAT was defined as the amount of enzyme required to degrade 1 μmol of H_2O_2 min^{-1} mg^{-1} of protein (Aebi 1984).

Nutrient and hydrolyzed amino acid concentration measurements

The concentrations of K^+, Na^+ and Ca^{2+} were determined using atomic absorption spectroscopy, as described by Chen et al. (2010). Leaf samples were dried at 80 °C for 48 h, ground to powder and passed through a 100-mesh screen. The samples were extracted overnight with HCl at 37 °C. After centrifugation at 10 000 *g* for 10 min, the supernatants were diluted, and K^+, Na^+ and Ca^{2+} contents were determined using an atomic absorption spectrophotometer (Analyst 300; Perkin Elmer, Frankfurt, Germany).

For estimation of the hydrolyzed amino acid concentrations, dry leaf powder (0.1 g) was transferred to a 20-ml hydrolysis tube, and 10 ml 6 mol l^{-1} hydrochloric acids was added and evacuated. The hydrolysis tube was then sealed and transferred to a constant-temperature drier at 110 ± 2 °C, and hydrolysis was carried out for 22 h. The tube was removed from the dryer and cooled, and the hydrolysis liquid was filtered and transferred to a 50-ml volumetric flask and diluted with deionized water to scale. Then, 1 ml of the diluted hydrolysis liquid was drawn into a 5-ml volumetric flask and dried at 40-50 °C using a vacuum drier. The residue was dissolved in 1 ml sodium citrate-hydrochloric acid buffer (pH 2.2), and the content and composition of amino acids were determined using an L-8800 automatic amino acid analyzer (Hitachi, Tokyo, Japan).

RNA isolation, DEG library preparation and data analysis

RNA extraction and sequencing were completed by ANOROAD gene technology (Beijing) Co., Ltd. Four digital gene expression libraries, including two control treatment libraries (*P. cathayana* males and females exposed to total nutrient solution, MC and FC) and two K^+-deficit treatment libraries (*P. cathayana* males and females exposed to K^+-deficit nutrient solution, MK and FK) were prepared. Leaves were fast frozen prior to RNA extraction. Total RNA was extracted from three biological replicates using E.Z.N.A.™ Plant RNA Kit (Omega Bio-Tek, Doraville, GA) according to the manufacturer's instructions. Residual genomic DNA was removed with DNase I, and the RNA integrity was checked using an Agilent 2100 Bioanalyzer (Agilent Technologies, Santa Clara, CA). The RNA purity was detected using a Kaiao K5500 microspectrophotometer. Firstly, the mRNA in the samples was adsorbed and purified using Oligo (dT) magnetic beads, and fragmentation buffer was added to the resulting mRNA to break its fragments into short fragments. Then, reverse transcription was performed to generate synthetic double-stranded cDNA. The first strand of cDNA was synthesized by random hexamers with a fragment of mRNA as template, and the second chain of cDNA was synthesized by adding buffer, dNTPs, RNase H and DNA polymerase I. QiaQuick PCR kit was used to purify and add EB buffer to remove the end of the repair, then plus the base A and sequencing connector. Next, agarose gel electrophoresis was used to recover the target fragments, and PCR amplification was performed as well to complete the whole library preparation. At last, the completed libraries were sequenced by Illumina HiSeq™ 2000, and the sequencing strategy was SE50 sequencing.

The original image data generated by the sequencer is converted into sequence data by base calling. Some of the original sequences with adaptor sequences, or contain a small number of low quality sequences were removed impurities and get clean reads through a series of data processing. Data processing steps: 1) remove adaptor containing reads, 2) removal of N with a ratio greater than 10% reads, 3) removal of low quality reads (quality value $Q \leq 5$ base accounted for more than 50% of read).

The depth of sequencing was closely related to the level and accuracy of gene expression. In order to explore the effect of sequencing depth on gene expression analysis, the expression was calculated by FPKM method:

$$\mathrm{FPKM} = \frac{10^6 * \mathrm{F}}{\frac{\mathrm{NL}}{10^3}}$$

FPKM (A) is the expression of the gene A, F is the only fragment number to the gene A, N is the only reference to the total number of reads gene, L is the base of the gene A. The RPKM method can eliminate the influence of the gene length and the amount of sequencing on the gene expression. The calculated gene expression can be directly used to compare among different products (Anders et al. 2010).

In order to explore the effect of K^+ deficiency on *P. cathayana* males and females at the transcriptional level, DEGseq software (Trapnel et al. 2013) was used to compare samples. RPKM method was used to calculate the expression level of unigenes and analyze the DEGs. Sequences were aligned against the poplar genome (*Populus trichocarpa* v3.0, DOE-JGI, www.phytozome.net/poplar). Both *P. cathayana* and *P. trichocarpa* belong to Tacamahaca (genus *Populus*, family Salicaceae). Among the *Populus* species only the genome of *P. trichocarpa* are available. Therefore, the genome of *P. trichocarpa* was selected as the reference genome. $|\log_2 \text{ratio}| \geq 1$ and $p \leq 0.01$ as selected criteria can be more accurate and reliable identification of DEGs. In this study, DEGs involved in metabolic processes were analyzed using MapMan (version 3.6.0RC1; http://www.gabipd.de/projects/MapMan/) according to the standard protocol (Usadel et al. 2005). The database of Kyoto Encyclopedia of Genes and Genomes (KEGG) was used to further study the complex biological pathway of unigenes (Kanehisa et al. 2008).

Quantitative real-time polymerase chain reaction

cDNA was synthesized from total RNA using a TUREscript 1st Strand cDNA Synthesis Kit (Germany) according to the manufacturer's recommendation, and real-time PCR was conducted using a fluorescence quantitative gradient PCR instrument (Analytik Jena-qTOWER2.2, Germany). For each reaction, 1 µl diluted cDNA (equivalent to 25 ng of total RNA) was mixed with 5 µl 2×SYBR® Green Supermix (DBI, Germany) and 100 nmol each of forward and reverse primers in a final volume of 10 µl. Adopting the Pfaffl's method (Pfaffl 2004), the relative expression of target genes in each sample was calculated using the software qPCRsoft3.0. The gene-specific primers utilized are presented in Appendix S1. Ubiquitin conjugating enzyme (NCBI accession number: XM_002307243.1) were used as reference genes. The qRT-PCR was performed in triplicate. Gene expression was evaluated using the comparative cycle threshold method, and the data were expressed as mean ± SE.

Statistical analyses

All data were analyzed using the software Statistical Package for the Social Sciences (SPSS Inc., Chicago, IL) version 17.0. Two-way ANOVA was used to assess sex × K interaction effects. Prior to analysis, the data were checked for normality and homogeneity of variance. Individual differences among means were determined using the Tukey's test of one-way ANOVA at a significance level of $p < 0.05$. Mean values and standard errors were determined for each variable.

Results

Sexual differences in gas exchange, chlorophyll content and chlorophyll fluorescence

Under K^+-deficient conditions, the values of P_n, F_v/F_m, *qN*, *qP*, *Chl b*, *TChl* and *Caro* were decreased significantly in *P. cathayana* females only. Conversely, g_s and *E* were increased but significantly in *P. cathayana* males only (Table 1). Significant interaction effects related to sex were found for these physiological parameters under K^+-deficient conditions. Compared with the control groups, the interaction effects between K^+ deficiency and sex were significant for *TChl*, *Caro* and *qN*, but neither sex nor K^+ effect was significant with regard to C_i, *Chl a* or *Yield* values.

Sexual differences in the hydrolyzed amino acid concentration

Under both control and K^+-deficient conditions, the concentrations of total amino acids (TAA) and individual amino acids were higher in *P. cathayana* females than in males, except for glycine. Compared with controls, K^+ deficiency caused significant increase of leucine, tyrosine, and arginine concentrations and decrease of threonine, glycine and lysine concentrations in *P. cathayana* females. In males, K^+ deficiency significantly increased the concentrations of threonine, serine, glutamic acid, isoleucine, leucine and glycine but decreased arginine and valine concentrations. Moreover, the interaction effects between K^+ deficiency and sex were significant for threonine, serine, glutamic acid, glycine, alanine, lysine and arginine (Table 2).

Sexual differences in nutrient concentrations and antioxidant enzyme activities

K^+ deficiency significantly decreased foliar K^+ and Na^+ concentrations and the K^+: Na^+ ratio but increased the Ca^{2+} concentration in both sexes (Fig. 1). Between the sexes, *P. cathayana* males had higher K^+ and Na^+ concentrations under control conditions, but there was no sex-related difference under K^+-deficient conditions. As shown in Fig. 2, there was no significant sexual difference of SOD, CAT, APX and POD activities under K^+-deficient conditions. *P. cathayana* males exhibited higher activities of CAT and POD under both control and K^+-deficient conditions.

Sexually different DEGs induced by potassium deficiency

Four DEG libraries were sequenced using Illumina-Solexa technology. Each library was sequenced twice. The average number of original reads per library was greater than 5 million, and the number of clean reads per library ranged from approximately 4.60 to 6.26 million (Appendix S2). The proportion of Q30 was more than 97% which showed a high sequencing accuracy. According to the selected criteria of $p \leq 0.01$ and $|\log_2 \text{ratio}| \geq 1$, we found 111 and 181 DEGs, of which 79 and 119 DEGs were increased and 32 and 62 DEGs were decreased in *P. cathayana* males and females, respectively (Fig. 3). Among of these, 19 DEGs were commonly altered in both sexes. The detailed information of DEGs is shown in Appendix S3. Analysis of these DGEs using MapMan software, we found that most of the

DEGs in *P. cathayana* males are mainly involved in hormone metabolism, RNA regulation of transcription, the cell wall, lipid metabolism, stress and GDSL-motif lipase; those in *P. cathayana* females are largely related to the cell wall, secondary metabolism, stress and transport. Additionally, to confirm the accuracy of the transcriptional profiling, eight genes (potri.014g149700.1, potri.002g014000.1, potri.005g096400.1, potri.013g113200.1, potri.013g102400.1, potri.t170400.1, potri.014g146700.1, potri.012g002500.1) were randomly selected for qRT-PCR analysis. The qRT-PCR results were all consistent with the transcriptional data (Appendix S7), suggesting a good reliability of these data.

To identify possible biological pathways that govern the responses of DEGs, we also matched DEGs to terms in the KEGG database for both sexes of *P. cathayana* under K^+-deficient conditions. The results revealed 25 pathways (Appendix S4). Most of the pathways were sex-specific, except for 4 pathways found in both sexes: protein metabolic processes, plant-pathogen interaction, amino sugar and nucleotide sugar metabolism and plant hormone signal transduction.

Sexually differential DEGs involved in photosynthesis, stress and redox

According to the MapMan analysis, 2 (encoding a subunit of ATPase complex CF0 and ATPase alpha subunit) and 10 DEGs are involved in photosynthesis in males and females, respectively (Table 3). In females, these DEGs are predominantly involved in the photosystem reaction center and the Calvin cycle (Fig. 4). Under the category of stress response, 8 and 14 DEGs were found in *P. cathayana* males and females, respectively (Table 3 and Fig. 5). All these DEGs were up-regulated and sex-specific, except for two 17.6-kDa small heat shock proteins (sHSPs) in females. Additionally, DEGs of the redox category induced by K^+ deficiency were also sex-specific. Two genes that encode copper/zinc superoxide dismutase 2 were up-regulated in *P. cathayana* males, and 2 genes, ascorbate peroxidase and an oxygen transporter, were down-regulated in females. A gene encoding a glutaredoxin family protein was down-regulated in males but up-regulated in females.

Sexually different DEGs involved in signaling, transport and the cell wall

There were 2 and 4 DEGs related to signaling in *P. cathayana* males and females, respectively (Table 3 and Fig. 5). Aside for genes encoding calcium-binding proteins being down-regulated in males (potri.001g471100.3) and females (potri.005g259900.1), the other genes were sex-specific. For example, the gene encoding G-protein was up-regulated in *P. cathayana* males only, and genes encoding a calcium-binding protein, a Ras-related GTP-binding protein and a phototropic-responsive NPH3 family protein were up-regulated in *P. cathayana* females only. Interestingly, more genes in the category of

transport proteins but fewer cell wall-related genes were up-regulated in *P. cathayana* females than in males.

Sexually differential DEGs involved in gene expression regulation

According to MapMan analysis, many sex-specific DEGs under K^+-deficient conditions are related to the categories of regulation of transcription and protein synthesis, degradation and posttranslational modification (Appendix S5 and S6). DEGs involved in transcriptional regulation are involved in a wide range of regulated processes, such as DNA binding, protein binding and transcription factor. Almost all genes encoding ribosomal proteins were down-regulated but those involved in posttranslational modifications were up-regulated in both sexes. Sexually differential DEGs in these processes were also found. However, changes in genes involved in protein degradation were complex. For example, a gene encoding a matrixin family protein was down-regulated in *P. cathayana* males and up-regulated in females, but the gene encoding serine-type endopeptidase was down-regulated in both sexes. Two DEGs (scpl33 and a gene encoding a matrixin family protein) were up-regulated in males, and 4 DEGs (*e.g.*, genes encoding zinc finger family and zinc ion-binding proteins) were up-regulated in females.

Discussion

K^+ deficiency caused a visible gender-specific decrease of photosynthesis in *P. cathayana*. Difference in chlorophyll pigment concentrations is an important reason for sex-specific photosynthetic activity when plants suffer from nutrient (*e.g.*, nitrogen, phosphorus and iron) deficiencies (Zhang et al. 2014, 2016b). In this study, we found that K^+-deficient females had reduced *Chl b*, *TChl* and *Caro* concentrations compared to K^+-deficient males, which may be responsible for the reduced net photosynthetic rate. Transcriptomic data also revealed several sex-specific DEGs involved in chlorophyll pigment metabolic processes. It is known that *Chl b* reductase plays a key role in the degradation of light harvesting complex II (LHCII), which is the most abundant pigment protein complex in plants (Consoli et al. 2005, Horie et al. 2009). In this study, a gene (SDR) encoding *Chl b* reductase was down-regulated in K^+-deficient *P. cathayana* females only, indicating a greater decline in *Chl b* and a lower photosynthetic rate. In addition, the NCED4 gene, which participates in *Caro* biosynthesis, was down-regulated in *P. cathayana* females only. Ostroumov et al. (2013) indicated that a dark-state *Caro* pigment is involved in the process of photosynthesis and that the energy absorbed by it could be effectively transferred to chlorophyll. Additionally, several genes encoding the Rubisco large subunit were down-regulated only in K^+-deficient females, indicating that Rubisco synthesis was blocked, which further led to a greater decrease in the photosynthetic rate by affecting CO_2 assimilation. Therefore, sexually differential gene expression in photosynthetic process might responsible for sexual variation in the photosynthetic rate.

Ca^{2+} is a ubiquitous second messenger that participates in signal transduction in plant cells, and free Ca^{2+} will be rapidly increased in the cytoplasm when plants suffer from stress (Luan et al. 2009, Tian et al. 2015). Our transcriptome data showed that a gene encoding calcium-binding protein was up-regulated in K^+-deficient *P. cathayana* males and that 2 genes related to Ca^{2+} exchange were up-regulated in K^+-deficient *P. cathayana* females. These findings may reflect a positive feedback of the increase of Ca^{2+} concentration in leaves under K^+-deficient stress. Proteins with an EF hand-shaped structure play key roles in Ca^{2+} regulation, and K^+ outward rectifying channel 1 (KCO1) has such a Ca^{2+}-binding protein EF hand-shaped structure (Czempinski et al. 1997). In this study, a gene encoding protein with a similar EF hand-shaped structure of the Ca^{2+}-binding protein family was detected in *P. cathayana* males only. While the gene CML38, encoding a calcium-binding EF-hand protein family member, was down-regulated in females only. These results indicate there are sexually different changes in signal transduction under K^+-deficient conditions. Pathway-based KEGG analysis helps us to further understand the biological processes and signal transduction. Appendix S8 illustrates the DEGs involved in the plant hormone signal transduction pathway. Interestingly, SAUR and NPR1 were up-regulated in *P. cathayana* females, ultimately affecting cell enlargement, plant growth and disease resistance. In *P. cathayana* males, PP2C and CYCD3 were up-regulated, ultimately affecting stomatal closure (decrease

in stomatal conductance) and cell division. Therefore, *P. cathayana* males and females might adopt different strategies in response to K^+ deficiency.

Evidences showed that various biotic and abiotic stresses including K^+ deficiency could lead to an overproduction of reactive oxygen species (ROS) in plants, which further resulted in an oxidative stress (Desikan et al. 2001, Mittler 2006, Wang and Wu 2010). To protect against oxidative damage, plants possess efficient enzymatic and non-enzymatic antioxidant defense systems to scavenge ROS (Miller et al. 2010, Bose et al. 2014). Although the gene expression of Cu/Zn-SOD was up-regulated in *P. cathayana* males by K^+ deficiency, we found little change of antioxidase activity. There may be two reasons for this phenomenon. One, antioxidases comprise the primary enzymatic defense system, and their activities change dynamically with treatment time. Hafsi et al. (2011) found that SOD, GPX and APX activities were increased in *Hordeum maritimum* under 2 weeks of K^+ deficiency, whereas Gong et al. (2011) reported that these activities significantly decreased with 35 days of K^+ deficiency. Two, to perform their biological functions, antioxidant enzymes and their isoenzymes must coordinate metal ions. For example, SODs in plant cells detoxify superoxide anion free radicals by formation of H_2O_2 and may contain Cu^{2+}, Zn^{2+} or Fe^{2+} as mental components (Zhang et al. 2016b). However, K^+ deficiency disrupts the ionic equilibrium and alters metal ion concentrations in plant tissues (Leigh and Storey 1993). Therefore, although the gene expression or abundance of SOD is increased, its activity might be limited by the availability of metal ions. Interestingly, we also found some DEGs to be non-enzymatic antioxidants. Heat shock proteins (HSPs) are typical non-enzymatic antioxidants triggered by environmental stresses (Vanderauwera et al. 2005). In this study, 2 and 9 HSPs were up-regulated in *P. cathayana* males and females by K^+ deficiency, respectively. Accumulation of HSPs in poplars may be an essential response with a role in eliminating H_2O_2 under K^+-deficient conditions. Additionally, the gene encoding GST (GSTU7 and GSTU25), which is involved in the glutathione metabolism pathway, was up-regulated in males by K^+ deficiency. This was consistent with the increase of glutamic acid, cysteine and glycine concentrations in K^+-deficient males only (Table 2).

Sexually differential DEGs related to secondary metabolites were also found. For instance, genes encoding enzymes participating in terpenoid pathways were up-regulated in *P. cathayana* males, and those related to simple phenols were up-regulated in females. The best-known functions of terpenoids are adaptation to abiotic and biotic stresses, including herbivore and pathogen attack (Holopainen et al. 2013), and phenolic compounds are major contributors to the antioxidant properties in plants (Dudonné et al. 2009, Fares et al. 2010). Additionally, several DEGs encoding GDSL-motif lipase/hydrolase family proteins were up-regulated in *P. cathayana* males only, *e.g*., SFAR4, a GDSL-type esterase. SFAR4 plays an important role in fatty acid degradation (Huang et al. 2015), and its primary metabolites function in plant disease resistance (Bolton 2009). Pectin is a major constituent of the primary cell wall, and pectin hydrolysis will cause cells to separate from each other (Fry 2004, Harholt et al. 2010).

Pectin methyl esterase (PME) can modify the molecular organization of the pectin complex, with an essential role in regulating the mechanical properties of the cell wall (Micheli 2001). In this work, the gene encoding PME was down-regulated in males but up-regulated in females by K^+ deficiency. Genes encoding transeliminase and pectin methyl esterase inhibitor (PMEI) were up-regulated in *P. cathayana* males only. PMEI can effectively inhibit the activity of PME in plants to protect the cell wall. These results suggest that K^+ deficiency probably causes less damage to pectin in the cell wall, with less injury to *P. cathayana* males than females.

Additionally, previous studies have shown that K^+-deficient plants could accumulate more Na^+ than K^+-sufficient plants (Gerardeaux et al. 2010, Shin and Adams 2014). However, in this study, we found that the Na^+ concentration was significantly decreased in both sexes with 10 week of K^+ deficiency. Terry et al. (1973) reported that after the K^+ supply was stopped, the concentration of Na^+ in the leaves first increased and then decreased. Tian et al. (2015) also found that the Na^+ concentration was significantly decreased in wheat seedlings after 15 days of K^+ deficiency. Therefore, we think that K^+ and Na^+ concentrations may change dynamically over time. Moreover, the K^+: Na^+ ratio in *P. cathayana* males was significantly higher than that of in females under K^+-deficient conditions, indicating that males have a better ability to maintain a K^+-Na^+ balance to resist K^+ deficiency.

In conclusion, our results indicate there were sexually differential responses to K^+ deficiency at both physiological and transcriptomic levels in *P. cathayana*. The DEGs caused by K^+ deficiency are mainly involved in photosynthesis, the cell wall, secondary metabolism, transport, stress responses, gene expression regulation and protein synthesis and degradation. Our transcriptomic data reveal that K^+ deficiency results in many DEGs involved in photosynthesis and gene expression regulation but fewer involved in secondary metabolism, stress responses and redox in females, suggesting that females are more susceptible to K^+ deficiency than males. These results provide new evidence that *P. cathayana* females and males have adopted sex-related molecular strategies in response to K^+ deficiency.

Author contributions

Qingquan Han had the main responsibility for data collection, analysis and writing, Haifeng Song had a significant contribution to data collection and analysis, Yanni Yang had significant contributions to data collection and experimental arrangements, Hao Jiang had a significant contribution to the interpretation of data and manuscript preparation, and Sheng Zhang (the corresponding author) had the overall responsibility for experimental design and project management.

Acknowledgements - This work was supported by the Excellent Young Scientist Program of the National Natural Science Foundation of China (NO. 31322014) and the Frontier Science Key Research Programs of CAS (QYZDB-SSW-DQC037).

References

Aebi H (1984) Catalase in vitro. Method Enzymol 105: 121-126

Anders S, Huber W (2010) Differential expression analysis for sequence count data. Genome Biol 11: R106

Arend M, Monshausen G, Wind C, Weisenseel MH, Fromm J (2004) Effect of potassium deficiency on the plasma membrane H^+-ATPase of the wood ray parenchyma in poplar. Plant Cell Environ 27: 1288-1296

Audic S, Claverie J (1997) The significance of digital gene expression profiles. Genome Res 7: 986-995

Bolton MD (2009) Primary metabolism and plant defense-fuel for the fire. Mol Plant Microbe In 22: 487-497

Bose J, Rodrigo-Moreno A, Shabala S (2014) ROS homeostasis in halophytes in the context of salinity stress tolerance. J Exp Bot 65: 2808-2837

Chance B, Maehly AC (1955) Assay of catalases and peroxidases. Method Enzymol 2: 764-775

Chen FG, Chen LH, Zhao HX, Korpelainen H, Li CY (2010) Sex-specific responses and tolerances of *Populus cathayana* to salinity. Physiol Plantarum 140: 163-173

Chen L, Han Y, Jiang H, Korpelainen H, Li CY (2011) Nitrogen nutrient status induces sexual differences in responses to cadmium in *Populus yunnanensis*. J Exp Bot 62: 5037-5050

Consoli E, Croce R, Dunlap DD, Finzi L (2005) Diffusion of light-harvesting complex II in the thylakoid membranes. Embo Rep 6: 782-786

Czempinski K, Zimmermann S, Ehrhardt T, Müller-Röber B (1997) New structure and function in plant K^+ channels: KCO1, an outward rectifier with a steep Ca^{2+} dependency. Embo J 16: 2565-2575

Desikan R, Hancock JT, Ichimura K, Shinozaki K, Neill SJ (2001) Harpin induces activation of the *Arabidopsis* MAP kinases *AtMPK4* and *AtMPK6*. Plant Physiol 126: 1579-1587

Dudonné S, Vitrac X, Coutière P, Woillez M, Mérillon JM (2009) Comparative study of antioxidant properties and total phenolic content of 30 plant extracts of industrial interest using DPPH, ABTS, FRAP, SOD, and ORAC assays. J Agr Food Chem 57: 1768-1774

Duan BL, Yang YQ, Lu YW, Korpelainen H, Berninger F, Li CY (2007) Interactions between water deficit, ABA, and provenances in *Picea asperata*. J Exp Bot 58: 3025-3036

Fares S, Oksanen E, Lännenpää M, Julkunen-Tiitto R, Loreto F (2010) Volatile emissions and phenolic compound concentrations along a vertical profile of *Populus nigra* leaves exposed to realistic ozone concentrations. Photosynth Res 104: 61-74

Feng L, Jiang H, Zhang YB, Zhang S (2014) Sexual differences in defensive and protective mechanisms of *Populus cathayana* exposed to high UV-B radiation and low soil nutrient status. Physiol Plantarum 151: 434-445

Fry SC (2004) Primary cell wall metabolism: tracking the careers of wall polymers in living plant cells. New Phytol 161: 641-675

Gerardeaux E, Jordan-Meille L, Constantin J, Pellerin S, Dingkuhn M (2010) Changes in plant morphology and dry matter partitioning caused by potassium deficiency in *Gossypium hirsutum* (L.). Environ Exp Bot 67: 451-459

Gong XL, Liu C, Zhou M, Hong MM, Luo LY, Wang L, Wang Y, Cai JW, Gong SJ, Hong FS (2011) Oxidative damages of maize seedlings caused by exposure to a combination of potassium deficiency and salt stress. Plant Soil 340: 443-452

Hafsi C, Romero-Puertas MC, del Río LA, Abdelly C, Sandalio LM (2011) Antioxidative response of *Hordeum maritimum* L. to potassium deficiency. Acta Physiol Plant 33: 193-202

Harholt J, Suttangkakul A, Scheller HV (2010) Biosynthesis of pectin. Plant Physiol 153: 384-395

Holopainen JK, Himanen SJ, Yuan JS, Chen F, Stewart Jr CN (2013) Ecological functions of terpenoids in changing climates. Natural Products, Springer Berlin Heidelberg, pp 2913-2940

Horie Y, Ito H, Kusaba M, Tanaka R, Tanaka A (2009) Participation of chlorophyll b reductase in the initial step of the degradation of light-harvesting chlorophyll a/b-protein complexes in *Arabidopsis*. J Biol Chem 284: 17449-17456.

Houman F, Godbold DL, Majcherczyk A, Wang SS, Hüttermann A (1991) Polyamines in leaves and roots of *Populus maximowiczii* grown in differing levels of potassium and phosphorus. Can J Forest Res 21: 1748-1751

Huang LM, Lai CP, Chen LFO, Chan MT, Shaw JF (2015) *Arabidopsis* SFAR4 is a novel GDSL-type esterase involved in fatty acid degradation and glucose tolerance. Bot Stud 56: 1-12

Jin SH, Huang JQ, Li XQ, Zheng BS, Wu JS, Wang ZJ, Liu GH, Chen M (2011) Effects of potassium supply on limitations of photosynthesis by mesophyll diffusion conductance in *Carya cathayensis*. Tree Physiol 31: 1142-1151

Kanehisa M, Araki M, Goto S, Hattori M, Hirakawa M, Itoh M, Katayama T, Kawashima S, Okuda S, Tokimatsu T, Yamanishi Y (2008) KEGG for linking genomes to life and the environment. Nucleic Acids Res 36 (Database issue): D480-D484

Kim MJ, Ruzicka D, Shin R, Schachtman DP (2012) The *Arabidopsis* AP2/ERF transcription factor RAP2.11 modulates plant response to low-potassium conditions. Mol Plant 5: 1042-1057

Lee KJ, Kim TY (2009) Interaction between potassium and ozone in biomass production and resistance to ozone of potted-cuttings of *Populus trichocarpa* and *P. trichocarpa* × *deltoides*. Forest Sci Tech 5: 1-9

Leigh RA, Storey R (1993) Intercellular compartmentation of ions in barley leaves in relation to potassium nutrition and salinity. J Exp Bot 44: 755-762

Li Q, Fritz E, Li TQ, Hüttermann A (1990) X-ray microananlysis of ion contents in roots of *Populus maximowiczii* grown under potassium and phosphorus deficiency. J Plant Physiol 136: 61-65

Lu ZF, Lu JW, Pan YH, Lu PP, Li XK, Cong RH, Ren T (2016) Anatomical variation of mesophyll conductance under potassium deficiency has a vital role in determining leaf photosynthesis. Plant Cell Environ 39: 2428-2439

Luan S, Lan WZ, Lee SC (2009) Potassium nutrition, sodium toxicity, and calcium signaling: connections through the CBL-CIPK network. Curr Opin Plant Biol 12: 339-346

Ma TL, Wu WH, Wang Y (2012) Transcriptome analysis of rice root responses to potassium deficiency. BMC Plant Biol 12: 161

Micheli F (2001) Pectin methylesterases: cell wall enzymes with important roles in plant physiology. Trends Plant Sci 6: 414-419

Miller G, Suzuki N, Ciftci-Yilmaz S, Mittler R (2010) Reactive oxygen species homeostasis and signalling during drought and salinity stresses. Plant Cell Environ 33: 453-467

Mittler R (2006) Abiotic stress, the field environment and stress combination. Trends Plant Sci 11: 15-19

Ostroumov EE, Mulvaney RM, Cogdell RJ, Scholes GD (2013) Broadband 2D electronic spectroscopy reveals a carotenoid dark state in purple bacteria. Science 340: 52-56

Porra RJ, Thompson WA, Kriedemann PE (1989) Determination of accurate extinction coefficients and simultaneous equations for assaying chlorophylls a and b extracted with four different solvents: verification of the concentration of chlorophyll standards by atomic absorption spectroscopy. BBA – Bioenergetics 975: 384-394

Pfaffl MW (2004) Quantification strategies in real-time PCR. In: Bustin SA (ed) A-Z of quantitative PCR. International University Line Biotechnology Series, La Jolla, pp 87-112

Shin R, Adams E (2014) Transport, signalling and homeostasis of potassium and sodium in plants. J Integr Plant Biol 56: 231-249

Terry N, Ulrich A (1973) Effects of potassium deficiency on the photosynthesis and respiration of leaves of sugar beet under conditions of low sodium supply. Plant Physiol 51: 1099-1101

Tian X, He M, Wang Z, Zhang J, Song Y, He Z, Dong Y (2015) Application of nitric oxide and calcium nitrate enhances tolerance of wheat seedlings to salt stress. Plant Growth Regul 77: 343-356

Trapnell C, Hendrickson DG, Sauvageau M, Goff L, Rinn JL, Pachter L (2013) Differential analysis of gene regulation at transcript resolution with RNA-seq. Nat Biotechnol 31: 46-53

Usadel B, Nagel A, Thimm O, Redestig H, Blaesing OE, Palacios-Rojas N, Selbig J, Hannemann J, Piques MC, Steinhauser D, Scheible WR, Gibon Y, Morcuende R, Weicht D, Meyer S, Stitt M (2005) Extension of the visualization tool MapMan to allow statistical analysis of arrays, display of coresponding genes, and comparison with known responses. Plant Physiol 138: 1195-1204

Vanderauwera S, Zimmermann P, Rombauts S, Vandenabeele S, Langebartels C, Gruissem W, Inzé D, Van Breusegem F (2005) Genome-wide analysis of hydrogen peroxide-regulated gene expression in Arabidopsis reveals a high light-induced transcriptional cluster involved in anthocyanin biosynthesis. Plant Physiol 139: 806-821

van Kooten O, Snel JFH (1990) The use of chlorophyll fluorescence nomenclature in plant stress physiology. Photosynth Res 25: 147-150

Wang C, Chen HF, Hao QN, Sha AH, Shan ZH, Chen LM, Zhou R, Zhi HJ, Zhou XA (2012) Transcript profile of the response of two soybean genotypes to potassium deficiency. PLoS One 7: e39856

Wang Y, Wu W (2010) Plant sensing and signaling in response to K^+-deficiency. Mol Plant 3: 280-287

Wang Y, Wu W (2013) Potassium transport and signaling in higher plants. Annu Rev Plant Biol 64: 451-476

Xu X, Yang F, Xiao XW, Zhang S, Korpelainen H, Li CY (2008) Sex-specific responses of *Populus cathayana* to drought and elevated temperatures. Plant Cell Environ 31: 850-860

Yang Y, Jiang H, Wang M, Korpelainen H, Li CY (2015) Male poplars have a stronger ability to balance growth and carbohydrate accumulation than do females in response to a short-term potassium deficiency. Physiol Plantarum 155: 400-413

Zhang S, Jiang H, Zhao HX, Korpelainen H, Li CY (2014) Sexually different physiological responses of *Populus cathayana* to nitrogen and phosphorus deficiencies. Tree Physiol 34: 343-354

Zhang S, Zhou R, Zhao HX, Korpelainen H, Li CY (2016a) iTRAQ-based quantitative proteomic analysis gives insight into sexually different metabolic processes of poplars under nitrogen and phosphorus deficiencies. Proteomics 16: 614-628

Zhang S, Zhang YB, Cao Y, Lei Y, Jiang H (2016b) Quantitative proteomic analysis reveals *Populus cathayana* females are more sensitive and respond more sophisticatedly to iron deficiency than males. J Proteome Res 15: 840-850

Zhao HX, Xu X, Zhang YB, Korpelainen H, Li CY (2011) Nitrogen deposition limits photosynthetic response to elevated CO_2 differentially in a dioecious species. Oecologia 165: 41-54

Figure legends

Fig. 1. The concentrations of K^+ (A), Na^+ (B) and Ca^{2+} (C), and the K^+ /Na^+ ratio (D) in *P. cathayana* females and males under control (white rectangles) and K^+-deficient (grey rectangles) conditions. Values are the mean ± SE (n=5). P_s, sex effect; P_k, K effect; $P_{S\times K}$, sex × K effect. Different letters above the symbols denote statistically significant differences between treatments at the $P < 0.05$ level according to the Tukey's test.

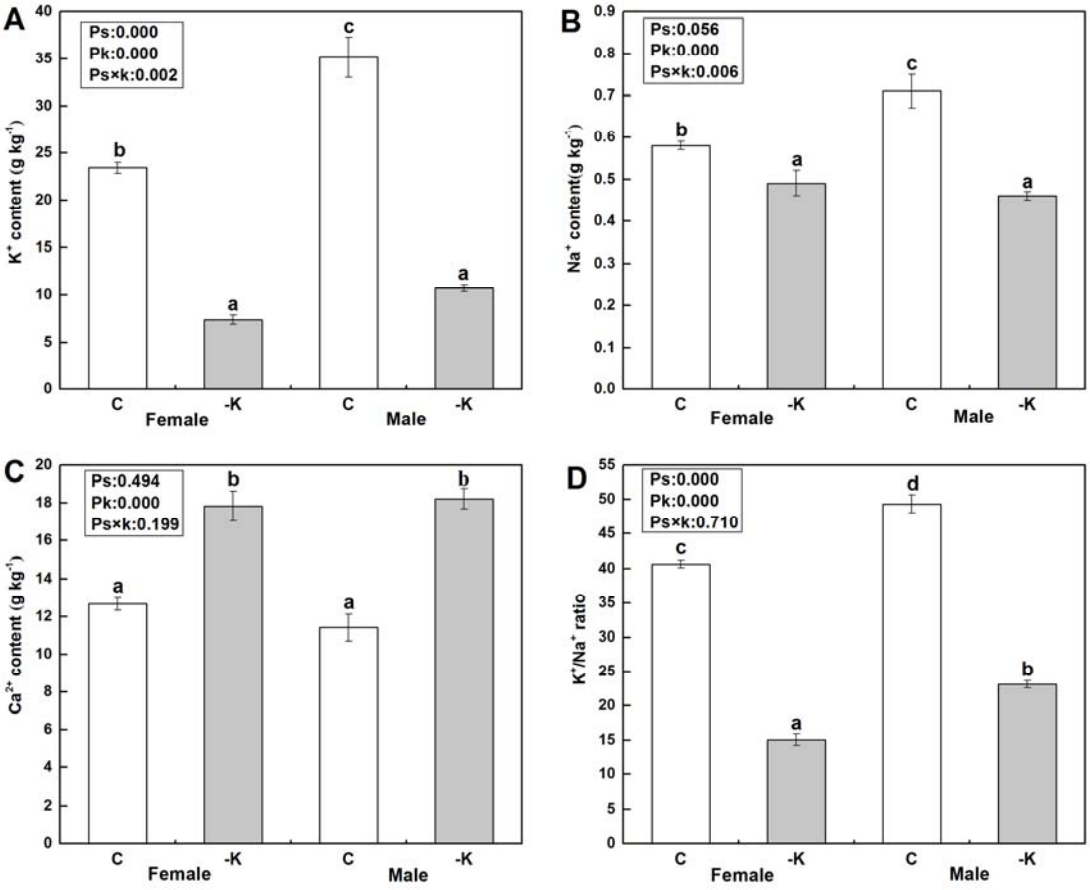

Fig. 2. Activities of SOD (A), CAT (B), APX (C) and POD (D) in *P. cathayana* females and males under control (white rectangles) and K^+-deficient (grey rectangles) conditions. Values are the mean ± SE (n=5). P_s, sex effect; P_k, K effect; $P_{S\times K}$, sex × K effect. Different letters above the symbols denote statistically significant differences between treatments at the $P < 0.05$ level according to the Tukey's test.

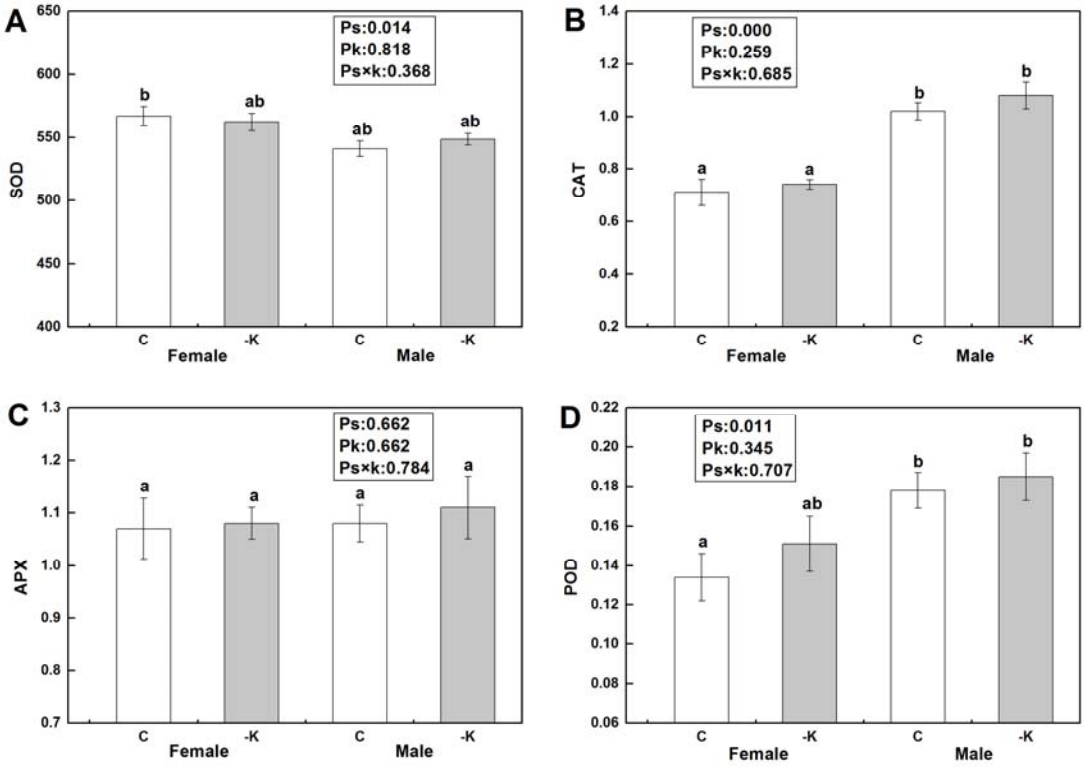

Fig. 3. Venn diagrams (A) and expression patterns (B) of DEGs in *P. cathayana* males and females under K^+-deficient conditions.

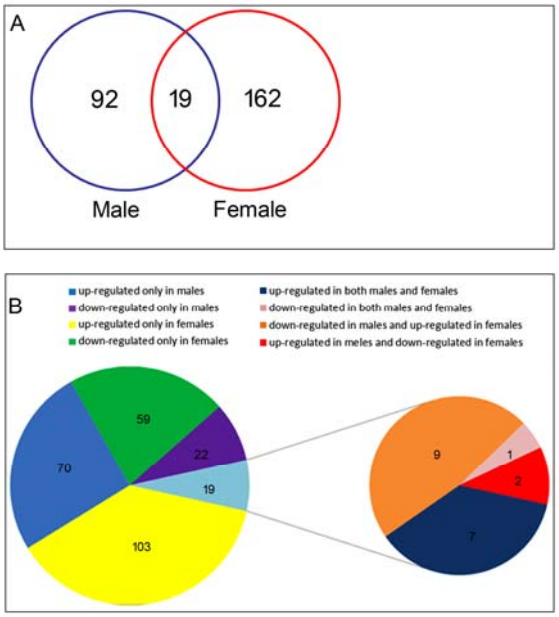

Fig. 4. DEGs involved in photosynthesis in *P. cathayana* males (A) and females (B) under K^+-deficient conditions. Red color, up-regulated; blue color, down-regulated.

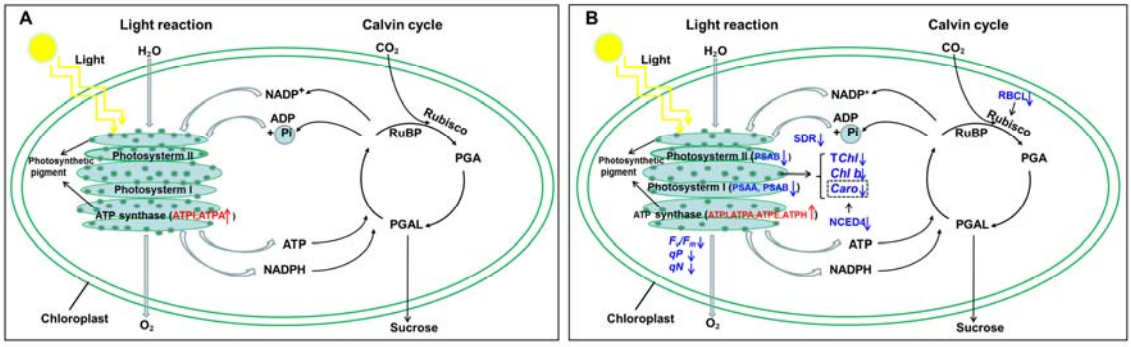

Fig. 5. An overview of DGEs assigned to "biotic stress" based on MapMan (version of 3.6.0RC1) analysis. (A) DEGs in *P. cathayana* males; (B) DEGs in *P. cathayana* females. The scale indicates DEGs significantly up-regulated (red) or down-regulated (blue) in response to K^+ deficiency.

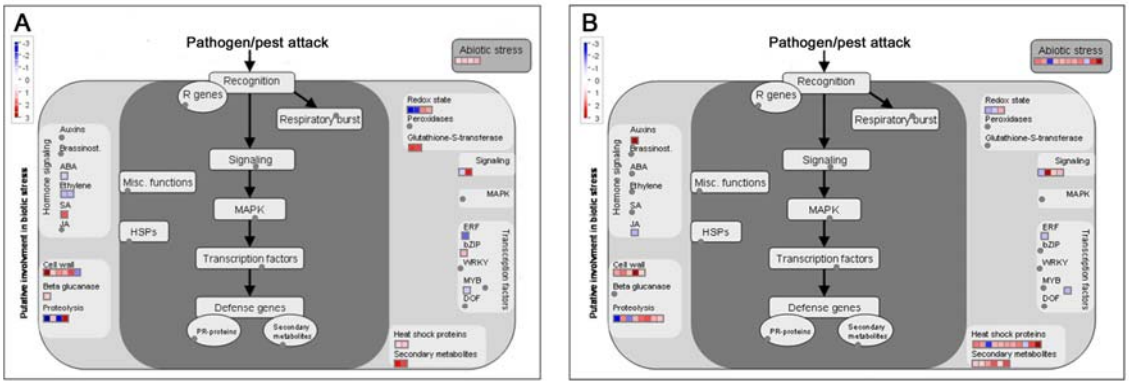

Supporting Information

Additional Supporting Information may be found in the online version of this article:

Appendix S1. Primer sequences of candidate genes used for validation in qRT-PCR.

Appendix S2. Basic information of digital gene expression profiling by Illumina-Solexa in *P. cathayana* females and males. MC, control males; MK, K^+-deficient males; FC, control females; FK, K^+-deficient females.

Appendix S3. DEGs induced by K^+ deficiency in *P. cathayana* males and females. MC, control males; MK, K^+-deficient males; FC, control females; FK, K^+-deficient females.

Appendix S4. DEGs involved in KEGG pathways. MC, control males; MK, K^+-deficient males; FC, control females; FK, K^+-deficient females.

Appendix S5. Functional categories and gene expression patterns of DEGs involved in regulation of transcription and secondary metabolism. MC, control males; MK, K^+-deficient males; FC, control females; FK, K^+-deficient females.

Appendix S6. Functional categories and gene expression patterns of DEGs involved in protein synthesis, degradation and posttranslational modification. MC, control males; MK, K^+-deficient males; FC, control females; FK, K^+-deficient females.

Appendix S7. qRT-PCR validations of DGE libraries data. A: potri.014g149700.1; B: potri.002g014000.1; C: potri.014g146700.1; D: potri.005g096400.1; E: potri.013g113200.1; F: potri.013g102400.1; G: potri.t170400.1; H: potri.012g002500.1

Appendix S8. A diagram of sex-specific DEGs involved in the plant hormone signal transduction pathway. The blue and red frames present DEGs in males and females under K^+ deficiency, respectively. Red font indicates up-regulated DEGs in males and females. Squares represent downstream target responses.

Table 1. Gas exchange parameters, chlorophyll pigment contents and chlorophyll fluorescence parameters of *P. cathayana* females and males under control (C) and K^+-deficient ($-K^+$) conditions. P_n, net photosynthesis rate; g_s, stomatal conductance; E, transpiration rate; C_i, intercellular CO_2 concentration; *Chl a*, chlorophyll a; *Chl b*, chlorophyll b; *TChl*, total chlorophyll, *Caro*, carotenoid; F_v/F_m, maximum efficiency of PSII; Yield, maximum effective quantum yield of PSII; *qP*, photochemical quenching coefficient; *qN*, non-photochemical quenching coefficient. Values are means ± SE (n = 5). Within a column, values followed by different letters are significantly different at the $P<0.05$ level according to the Tukey's test. The significance values of the factorial analysis (analysis of variance) for single and interactive effects are shown: P_S, sex effect; P_K, K effect; $P_{S\times K}$, sex × K effect.

Sex	K	P_n (μmol m^{-2} s^{-1})	g_s (mol m^{-2} s^{-1})	E (mmol m^{-2} s^{-1})	Ci (μmol m^{-2} s^{-1})	*Chl a* (ug g^{-1} FW)	*Chl b* (ug g^{-1} FW)	T*Chl* (ug g^{-1} FW)	*Caro* (ug g^{-1} FW)	F_v/F_m	Yield	*qP*	*qN*
Female	C	11.14±0.76b	0.36±0.09a	4.71±0.58a	289.70±8.36a	642.59±3.90a	703.70±18.44b	1359.71±13.43b	70.28±0.82c	0.77±0.00b	0.69±0.02c	0.95±0.01b	0.13±0.01b
	$-K^+$	8.23±0.09a	0.22±0.02a	3.74±0.50a	292.81±4.59a	644.47±1.02a	600.11±19.22a	1244.59±18.31a	57.25±1.94b	0.75±0.00a	0.64±0.02b	0.84±0.03a	0.09±0.00a
Male	C	13.42±0.69c	0.76±0.18b	9.81±1.47b	311.06±5.90a	640.85±1.38a	771.30±6.02c	1412.15±5.83c	41.59±0.76a	0.78±0.01b	0.69±0.02a	0.95±0.00b	0.13±0.01b
	$-K^+$	11.96±0.58bc	0.45±0.09a	6.15±0.57a	296.64±8.74a	639.42±2.96a	769.16±13.26c	1408.58±14.92c	38.60±1.38a	0.78±0.01b	0.70±0.03a	0.92±0.03b	0.16±0.02b
	P_S	0.011	0.066	0.008	0.253	0.011	0.025	0.000	0.000	0.005	0.143	0.093	0.014
	P_K	0.078	0.594	0.249	0.705	0.049	0.688	0.001	0.000	0.071	0.258	0.013	0.016
	$P_{S\times K}$	0.080	0.314	0.800	0.922	0.381	0.552	0.002	0.001	0.097	0.236	0.080	0.009

Table 2. Concentrations of hydrolysable amino acid of *P. cathayana* females and males under control (C) and K^+-deficient ($-K^+$) conditions. Values are means ± SE (n = 5). Within a column, values followed by different letters are significantly different at the $P<0.05$ level according to the Tukey's test. The significance values of the factorial analysis (analysis of variance) for single and interactive effects are shown: P_S, sex effect; P_K, K effect; $P_{S\times K}$, sex × K effect.

Hydrolysable amino acid	Female		Male				
(mg g^{-1} DW)	C	$-K^+$	C	$-K^+$	P_S	P_K	$P_{S\times K}$
Aspartic acid	0.42±0.010bc	0.44±0.012c	0.31±0.008a	0.36±0.040ab	0.001	0.132	0.502
Threonine	0.24±0.005d	0.21±0.006c	0.15±0.006a	0.17±0.009b	0.000	0.355	0.001
Serine	0.36±0.009c	0.31±0.009bc	0.21±0.012a	0.28±0.034b	0.001	0.607	0.007
Glutamic acid	0.47±0.017b	0.44±0.008b	0.31±0.008a	0.40±0.048b	0.003	0.268	0.038
Glycine	0.24±0.006c	0.20±0.005b	0.16±0.013a	0.22±0.012bc	0.013	0.274	0.000
Alanine	0.63±0.013b	0.67±0.017b	0.49±0.015a	0.43±0.040a	0.000	0.579	0.046
Valine	0.39±0.021b	0.35±0.025b	0.34±0.042b	0.24±0.025a	0.014	0.036	0.270
Isoleucine	0.13±0.009bc	0.14±0.005c	0.09±0.000a	0.12±0.009b	0.000	0.041	0.152
Leucine	0.30±0.013c	0.33±0.008d	0.19±0.005a	0.24±0.011b	0.000	0.001	0.219
Tyrosine	0.25±0.012b	0.32±0.014c	0.14±0.005a	0.18±0.019a	0.000	0.002	0.144
Phenylalanine	0.54±0.020b	0.53±0.015b	0.30±0.012a	0.35±0.025a	0.000	0.257	0.171
Lysine	0.26±0.006b	0.17±0.017a	0.16±0.005a	0.16±0.009a	0.000	0.001	0.002
Arginine	0.15±0.008b	0.25±0.005c	0.13±0.017b	0.08±0.009a	0.000	0.030	0.000
TAA	4.73±0.149b	4.78±0.095b	3.05±0.050a	3.53±0.295a	0.000	0.157	0.245

Table 3. Functional categories and gene-expression patterns of DEGs in *P. cathayana* females and males as affected by K^+ deficiency. MC, control males; FC, control females; MK, K^+-deficient males; FK, K^+-deficient females; "-" means no data was detected.

Populus gene model ID	Annotation and function description	Log_2 ratio	
		MK/MC	FK/FC
Photosynthesis			
potri.019g028600.1	Encodes a subunit of ATPase complex CF0 (ATPI)	1.12462	1.59976
potri.013g142800.1	Encodes the ATPase alpha subunit (ATPA)	1.15815	-
potri.005g154600.1	Encodes the ATPase alpha subunit (ATPA)	-	1.42965
potri.013g138000.1	Encodes the ATPase alpha subunit (ATPA)	-	1.23428
potri.007g054600.1	ATPase epsilon subunit (ATPE)	-	2.55544
potri.005g154900.1	ATPase III subunit (ATPH)	-	1.1865
potri.019g028100.1	Encodes psaA protein comprising the reaction center for photosystem I (PSAA)	-	-2.40663
potri.009g016300.1	Encodes the D1 subunit of photosystem I and II reaction centers (PSAB)	-	-2.35499
potri.t005800.1	Large subunit of rubisco (RBCL)	-	-2.0249
potri.t063100.1	Large subunit of rubisco (RBCL)	-	-1.75854
potri.012g062600.1	Large subunit of rubisco (RBCL)	-	-1.30139
Stress			
potri.009g148000.1	17.6 kDa class I small heat shock protein (HSP17.6)	1.16714	-1.17
potri.015g023900.1	Acidic endochitinase (CHIB1)	2.38115	-
potri.t094200.1	Osmotin 34 (OSM34)	1.75344	-
potri.015g039200.1	Pathogenesis-related protein/ thaumatin-like protein	1.59687	-
potri.009g028800.1	Osmotin-like protein	1.53596	-
potri.004g187400.1	17.6 kDa class I small heat shock protein (HSP17.6)	1.01043	-
potri.010g096000.1	MLP-like protein 423 (MLP423)	1.29901	-
potri.008g212300.1	Abiotic, unspecified	1.07234	-
potri.019g094100.1	Chitinase	-	2.01545

potri.006g188300.1	Glycosyl hydrolase family 18 protein	-	1.39183
potri.019g093900.1	Chitinase	-	1.18429
potri.001g221900.1	Pathogenesis-related thaumatin family protein	-	1.16117
potri.001g238700.1	Heat shock 17.4 kDa protein (HSP17.4)	-	2.08114
potri.013g018000.1	Luminal-binding protein 1	-	1.78325
potri.014g143400.4	DNAJ heat shock N-terminal domain-containing protein	-	1.76857
potri.006g093500.1	Heat shock 18.2 kDa protein (HSP18.2)	-	1.55317
potri.013g089200.1	22.0 kDa class IV heat shock protein precursor (HSP22.0)	-	1.5152
potri.012g022400.1	Heat shock 21 kDa protein (HSP21)	-	1.42874
potri.001g042700.1	Heat shock 70 kDa protein (HSP70)	-	1.32659
potri.001g192600.1	26.5 kDa class I small heat shock protein (HSP26.5)	-	1.29888
potri.009g049900.1	17.6 kDa class I small heat shock protein (HSP17.6)	-	-2.17958
Redox			
potri.004g216700.4	Copper/zinc superoxide dismutase 2 (CZSOD2)	1.69573	-
potri.009g005100.3	Copper/zinc superoxide dismutase 2 (CZSOD2)	1.47875	-
potri.014g134200.1	Glutaredoxin family protein	-2.50258	-
potri.008g099900.2	Antioxidant/ thioredoxin peroxidase	-2.22819	-
potri.002g208400.1	Glutaredoxin family protein	-	1.36064
potri.009g015400.7	Ascorbate peroxidase 1 (APX1)	-	-1.38274
potri.006g244300.1	Oxygen transporter	-	-1.11749
Signal transduction			
potri.011g061500.1	G-proteins	2.34199	-
potri.001g471100.3	Calcium ion binding	-1.01487	-
potri.003g066000.1	Calcium, GTP diphosphokinase	-	2.82826
potri.005g198800.2	Ras-related GTP-binding protein	-	1.12807
potri.002g242300.2	Phototropic-responsive NPH3 family protein	-	1.27929
potri.005g259900.1	Calcium-binding EF hand family protein (CML38)	-	-1.26444
Transport			
potri.004g176300.1	Plasma membrane intrinsic protein3 (PIP3)	1.28067	-

potri.018g053300.5	Cation transmembrane transporter	-1.16571	-
potri.014g146700.1	Amino acid transporter family protein	-	3.8983
potri.010g132300.1	EXS family protein	-	2.38789
potri.004g175700.1	High-affinity nickel-transport family protein	-	2.13227
potri.007g050600.1	Natural resistance-associated macrophage protein 3 (NRAMP3)	-	1.70943
potri.016g006500.1	Oligopeptide transporter 3 (OPT3)	-	3.64307
potri.014g036200.1	Nitrate transporter	-	2.57244
potri.006g006000.4	Oligopeptide transporter 3 (OPT3)	-	1.73339
potri.008g179500.1	ABC transporters and multidrug resistance systems	-	3.41205
potri.001g139600.1	P-glycoprotein 2 (PGP2)	-	1.28155
potri.016g115500.3	Calcium, cation exchanger 3 (CAX3)	-	1.04521
potri.002g107200.1	Antiporter/ drug transporter	-	1.8801
potri.001g076100.1	Cationic amino acid transporter 5 (CAT5)	-	-2.41017
potri.012g024700.3	Oligopeptide transporter	-	-1.04835
Cell wall			
potri.014g149700.1	Pectinesterase family protein (PME)	-1.65062	3.14643
potri.003g147600.1	Cellulase/ hydrolase (CEL2)	3.47752	-
potri.009g153900.2	Glycosyl hydrolase family 3 protein	1.12519	-
potri.002g238800.1	Pectate lyase family protein	1.6373	-
potri.011g093400.1	Pectate lyase family protein	1.38375	-
potri.009g006600.1	Xyloglucan endo-transglycosylase-related 8 (XTR8)	2.06956	-
potri.015g129400.1	Fasciclin-like arabinogalactan-protein (FLA12)	-	1.48383
potri.010g141400.1	Beta-xylosidase1 (BXL1)	-	1.80218
potri.018g098200.1	Expansin-like B2 precursor (EXLB2)	-	1.19144
potri.004g233900.3	Pectin acetylesterase	-	1.0541